SEMARAK ILMU PUBLISHING

CFD Letters

Journal homepage:
https://semarakilmu.com.my/journals/index.php/CFD_Letters/index
ISSN: 2180-1363

Experiments and Numerical Investigations for Heat Transfer from a Horizontal Plate via Forced Convection Using Pin Fins with Different Hole Numbers

Wadhah Hussein Abdulrazzaq Al Doori[1,*]

[1] Engineering of Petroleum Process College, University of Tikrit, Iraq

ARTICLE INFO

Article history:
Received 19 April 2022
Received in revised form 10 May 2022
Accepted 11 May 2022
Available online 23 August 2022

Keywords:

Enhancement heat transfer; Forced Convection; Pin Fins; Hole Numbers

ABSTRACT

Abstract This study focuses on perforated pin fin convection heat transfer. This study's goal is to see if perforated pin fins may help transmit heat. Perforation diameter and hole count are evaluated on each pin. The Nusselt number of perforated pins is 47% higher than solid pins, and it increases with perforation count. Unperforated solid pins have a 19% lower pressure drop. Using pin fins with circular holes as heat sinks, we examined forced convection heat transfer. There were circular perforations. They were conducted in a specifically designed laboratory. At low power, non-perforated fins lose 35 to 31 degrees Celsius, while perforated fins lose only 29.8 degrees (50 W). At 55°C, unperforated fins hit 55°C at full power, while perforated fins hit 38°C (600 W). The model had 16 pin fins and was built of aluminum alloy. When compared to solid pin fins, perforated fins were found to be the best way to improve heat transfer because they were 40% lighter and improved thermal efficiency by 30% to 85% by increasing the Nusselt number and the convective heat transfer coefficient and reducing the pressure gradient.

1. Introduction

Overheating can lead to system failure in a variety of industrial applications where heat generation is involved. Thus, heat transport has become a major concern in the science of thermodynamics. There are several ways to improve heat transfer from surfaces, including increasing their thermal performance, increasing their heat transfer coefficient, or doing both. Heat transfer was increased in most cases by using fins attached to walls and surfaces as extended surfaces [1]. To improve heat transfer between the primary surface and the surrounding fluid, fins (extended surfaces) are used in heat exchange devices [2].

Heat transfer enhancement devices, such as fins, have been around for a long time. When new technologies like anisotropic composite fins are developed, new design ideas emerge. Fin size optimization is essential in fin design because of the demand for unimportant and cost-effective fins. Fins must be designed to remove the greatest heat with the least amount of material while also taking

* *Corresponding author.*
E-mail address: wadhah.h.abdulrzzaq@tu.edu.iq

https://doi.org/10.37934/cfdl.14.9.114

into account the fin shape's ease of production [3]. Many studies have been conducted on fin shape optimization. It has been shown that removing some material from fins to create cavities, holes, slots, channels, or channels through the fin body can increase the heat transfer area or coefficient of heat transfer. A simple way to improve heat transfer is to use rough or uneven surfaces of different shapes and sizes [4][5].

There has been a lot of experimental and theoretical study on natural and forced convection heat transfer via a series of fins. Different investigators work on grooved channels, perforated fins, porous sleeves, obstructions with round and elongated holes, wooden porous material around staggered tube bundles, permeable fins, and so on. Prakash and Chethan [6] discovered that the heat transfer rate is higher in fins with two perforations in both natural and forced convection than in solid fins and fins with one perforation. When comparing solid fins and fins with one perforation to fins with two perforations in a staggered fin plate, the heat transfer rate is higher in fins with two holes in both natural and forced convection. It was shown that perforations increase fin area and heat transfer coefficients [1]. Conducted an experiment to see if circular perforations may increase natural convection heat transfer from rectangular fins. Heat transmission rates and coefficients rise as perforation numbers increased. Ehteshum *et al*.[7] conducted an experiment to determine the turbulent heat transfer capability of rectangular fin arrays with both solid and circular perforation. The size and quantity of circular perforations were changed in a horizontal wind tunnel with a forced draft fan. They also found that the possible values for the Reynolds number are between 6×10^4 and 25×10^4. Heat transfer, pressure drop, and efficiency are all significantly improved when perforated fins are used in place of solid fin arrays. This is in addition to the significant weight savings achieved by using perforated fins.

Choure *et al*. [8] and Jeng *et al*. [9] investigated heat transport in the finest perforated pin-fin heat sink experimentally and numerically. They determined that as the heat sink's holes grow in number and diameter so does the pressure drop across the heat sink. Pins with holes outperformed solid ones in all scenarios. Perforated pin fins required less pumping power than solid pins to obtain the same thermal performance. A bigger Nu is obtained by increasing the number and diameter of perforations. An increased hole diameter reduced thermal dissipation. Other researches on the thermal behavior of square and circular perforated fin arrays by forced convection has been investigated by Dhanawade *et al*. [10] and Al Doori [11]. Perforation sizes have been modified, with 10mm square, 8mm square, and 6mm square perforations were used for the analysis. They found that with increasing Reynolds numbers, the Nusselt numbers and thermal friction increased. The use of perforated fins increased the heat transfer and also reduced the weight, conserving material that ultimately decreased the expenditure on fin material.

By varying the perforation diameter from 4 to 12 mm and the inclination angles from 0-90°, Awasarmol and Pise [12] studied the heat transmission properties of a perforated pin fin array in natural convection condition. At a 45° angle, they discovered that fins with a perforation diameter of 12 mm allowed for more heat transfer. Bahadure and Gosavi [13] Investigated the thermal performance of a pin fin heat sink with a number of perforations constructed by copper, aluminum, and mild steel. They found that three holes gave better average heat transfer coefficient than solid, single, and two holes. Wu *et al*. [14] developed a heat sink model to predict the thermal efficiency of plate fin heat sinks. They developed correlations for forecasting the friction factor and Nusselt number for the case of Reynolds numbers less than 5000.

An investigation into the thermal hydraulic properties of perforated and solid rectangular blocks was conducted by Sara *et al*.[15]. According to study, the performance of solid and perforated blocks degrades as the Reynolds number increases. Few other studies used both experimental and

computational methods to assess the thermal performance of plate fin and plate-pin fin heat sinks [16,17]. Plate fins were shown to be more heat resistant than plate-pin fins.

From the above literature survey, we found that many studies have dealt with heat dissipated from heat sinks, however only a few deals with perforated pin fins dependent on forced convection mode. Therefore, in the current study, we aim to investigate forced convection heat transfer performance of solid and perforated pin fin heat sinks, both experimentally and numerically, as well as the heat sink performance of pin fins with different perforation diameters.

2. Experiment Method

A wind tunnel is used for this study's experimental system. An enclosed rectangular galvanized steel channel with a 1 m length and a cross-sectional area of 0.25m× 0.25m is used to evaluate the heat sink, as depicted in Fig. 1. The upstream section of the duct has a constant-speed air blower added to provide uniform airflow to the test unit. The fan has a constant velocity of 3 m/s. The inlet velocity can be measured using an anemometer at the rectangular channel's base. It is necessary to use a thermocouple to gauge the temperature of the air entering and exiting the heat sink. There are three side holes (8 mm in diameter by 80 mm in length) in an aluminum plate used as a heat sink for 200W of total power per element, with a 20 mm thickness and 100×100 mm2 dimensions. The base plate is fastened to 16 aluminum pin fins with a length of 100 mm. There are different numbers of holes with a diameter of 10 mm on each pin fin.

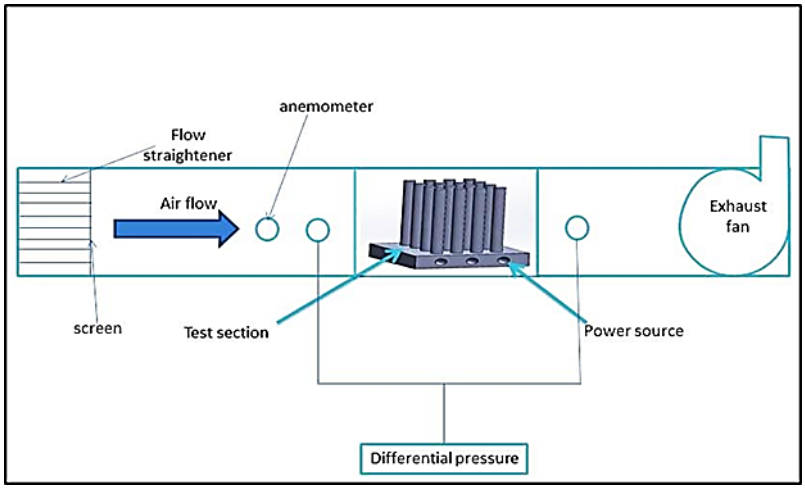

Fig. 1. The experimental setup diagram

Experimental works were carried out and the experimental data was collected using a data gathering system and the instruments and sensors. The flow of air through the tunnel was measured using a hot wire anemometer with a probe situated upstream of the test section. The pressure differential was measured with a digital manometer. All of the thermocouples were evenly scattered across the fin's surface as shown in Fig. 2. Other thermocouples were used to measure the temperatures of the input, outflow, and free stream air.

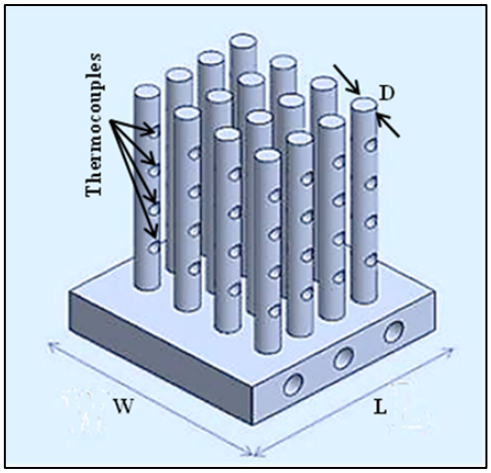

Fig. 2. Pin's dimensions and location of thermocouples

As shown schematically in figure 2, four thermocouples were installed in a single fin to monitor temperature fluctuations in the test rig produced by induced convection. There were four places where the thermocouples were evenly dispersed across the fin's surface. In all studies, steady state conditions were achieved after 1 hour and 30 minutes to 2 hours. The normal eccentricity of the two runs was determined to be the exact boundary for each heat subject. The thermistors on the fins' surfaces revealed that the differential between the base fins is negligible and falls below the 0.49°C limit in one batch of data. The thermocouples were put into the fin to measure the temperature of the free stream within 0.27°C of the average temperature in the inlet arrangement.

3. Application of Numerical Methods

The goal of this study is to offer a pin–fin model for a heat sink employing forced convection with solid and a variety of perforation numbers for the pin–fin heat sink system. SOLIDWORKS 2020 software was used to create the 3D models of the heat sinks, which were then loaded into the ANSYS FLUENT.16. There were three key steps in the computational fluid dynamics simulation: preprocessing, solver execution, and post-processing. Preprocessing is the stage in which the goal is determined and the computational element is created through the meshing process. The fins were modeled as aluminum with a specific heat flux input value at the base side surface of the array system, with fluid flow properties and the shape of the pin, as well as surrounding boundary conditions and numerical analysis models, to begin the solution process at the second stage. The solver model keeps running until it finds the solution's meeting point. The data will be delivered to the viewing phase after post-processing.

3.1 A model in physical form

An aluminum was employed as the material for the pin fins in this study. The pin fins for the various heat sink configurations were put on the base plate with dimensions W×L (0.25m x 0.25m) as shown in Figure 2. These geometries are arranged inside a channel in such a way that the zones before and after the investigated arrangement of pin fins heat transfer allow for the development of flows and the avoidance of reversed flows, respectively. In this work, solid, one, two, three, and four perforated numbers with a diameter of 10 mm were investigated. The pin fins for all variants are arranged in arrays across the base plate, as shown in Figure 3.

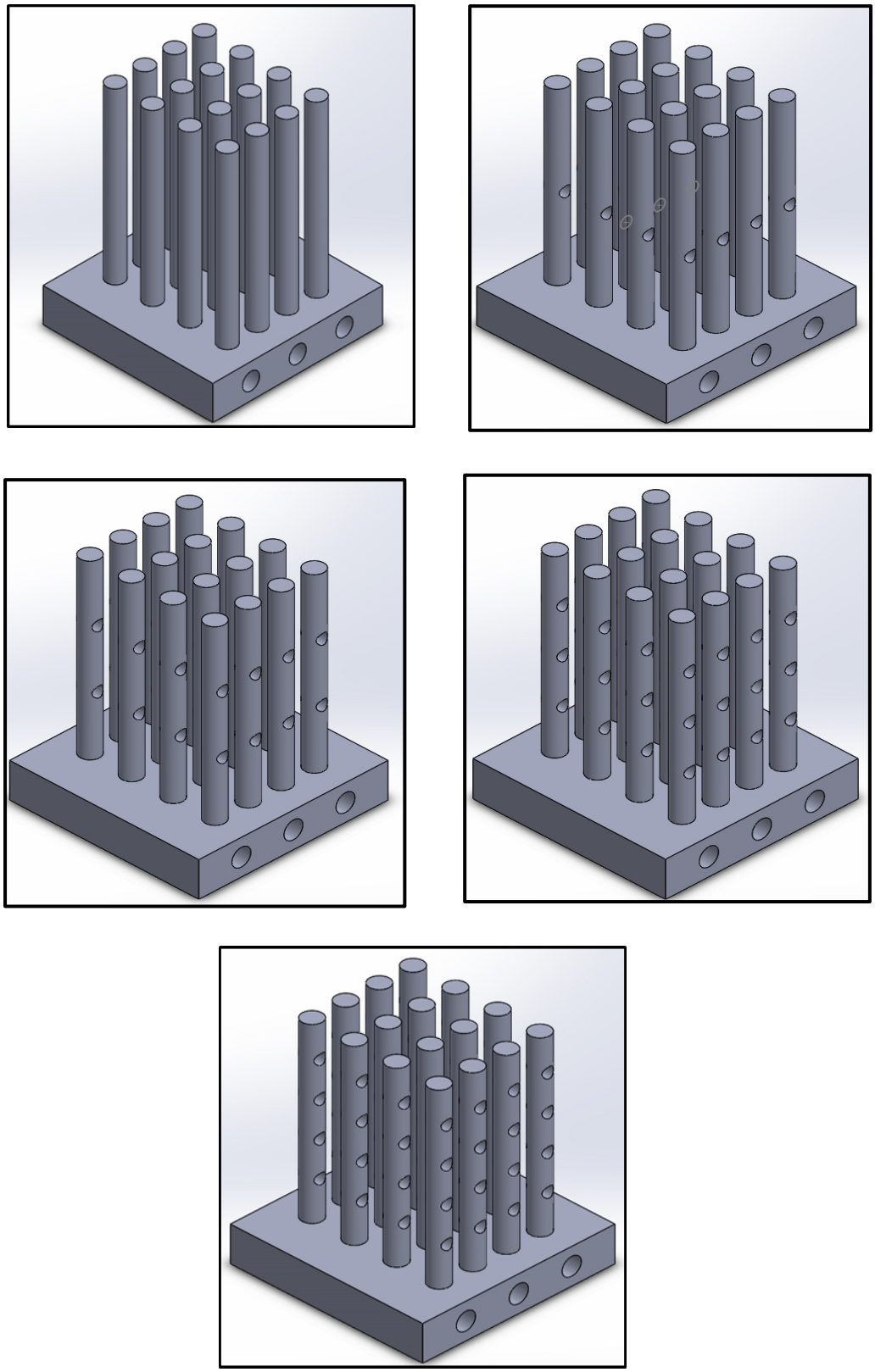

Fig. 3. An array of fins with different numbers of holes per fin

The continuity, momentum, and energy equations are used to predict the turbulent regime, incompressible flow, and heat transfer through pin fin heat sinks with forced convection. The fluid

flow conditions were also taken into account, including steady-state, turbulent, and incompressible air qualities. In addition, the thermos physical characteristics of air have been adjusted to remain constant. The effects of bouncing collisions and heat transmission from radiation are unimportant. In this case, the governing equations will be [18][19][3]:

Continuity equation is: $$\nabla \cdot (\rho u) = 0 \quad (1)$$

Momentum equation is: $$(\nabla \cdot u)\rho u = -\nabla p + \nabla \cdot \mu(\nabla u + (\nabla \cdot u)^2) \quad (2)$$

Energy equation is: $$\rho C_p u(\nabla T) = \nabla \cdot (k \nabla T) + Q \quad (3)$$

Heat sink system is shown as [20].

$$\nabla^2 T = 0 \quad (4)$$

The turbulence model employed in this paper is the *k–ε* standard. This model is frequently been used by researchers to predict turbulent flow in channels with obstructions, see for example [11]. The integral version of the governing equations is solved using the finite volume method with the continuum approach to solve the continuity, momentum, and energy equations. The mass, energy imbalance, and momentum convergence factors were all set to be less than 10^{-6} [21].

The temperature difference determines convective heat transfer, which is described by Newton's law as [22]:

$$Q_{conv.} = hA_s(T_b - T_\infty) \quad (5)$$

where h is the coefficient of heat transfer, T_b is the base temperature, and T_∞ is the temperature of the free stream. Equations (6), (7), and (8) represent the area of heat transmission for the various geometrical configurations employed in this study.

The solid pin, $$A_{sp} = wl + N(\pi DH) \quad (6)$$

The perforated pin, $$A_{pp} = wl + \pi N[(DH) + (ndD) - (nd/2)] \quad (7)$$

The solid fin $$A_{sf} = 2HNL + (N-1)SL \quad (8)$$

where W and L are the width and length of the heat sink, respectively, and H, D, and N are the height, diameter, and number of pin fins, respectively. Also, n is the number of perforations of diameter d on each pin fin.

Nusselt number can be used to assess whether convection or conduction is more prevalent. When assessing the transfer of heat, this is a vital factor to take into account [23], the average number of Nusselt is expressed as

$$\overline{Nu} = \frac{hL}{k} \quad (9)$$

On a smooth surface, the Nusselt number is as follows:

$$Nu_{sf} = 0.228Re^{0.731}Pr^{1/3} \text{ (For } 4000 \leq Re \leq 15000\text{)} \quad (10)$$

$$Nu = 0.683Re^{0.466}Pr^{1/3} \quad \text{(For } 4000 \leq Re \leq 40000\text{)} \quad (11)$$

The pressure drop is:

$$\Delta p = p_{in} - p_{out} \quad (12)$$

where P_{In} and P_{out} are the pressures at the channel's inlet and outlet flow channel respectively. The following equation can be used to determine the heat sink's thermal efficiency.

$$\eta = \frac{\overline{Nu}}{\Delta p} \quad (13)$$

The Reynolds number, Re, was calculated based on the hydraulic diameter of the channel (D_h).

$$Re = \frac{uD_h}{v} \quad (14)$$

where, u the mean air inlet velocity, D_h and v are the hydraulic diameter and the kinematic viscosity respectively.

3.2 Computational meshes

Figure 4 shows the distribution of mesh and computational domain for the present study. ANSYS.16 was used to create the model, with simulation procedure begins with designing the base plate, fin, and tunnel shapes. It is called the "mesh technique" because it begins with the design of the tunnel inlet, outlet, and wall, and each fin body is referred as an interface. The base fin serves to transport heat flux to the fin base. There is an entry level and an exit level, as well as a popular online surface far enough away from the slab faces to make these computations independent of border placement. On the other hand, the upstream plane may be slightly impacted by the addition of a boundary layer above the base boundary. This is necessary because of the uneven flow of the boxes' front borders. Our experimental works also based on these arrangements.

It is necessary to select grid point numbers in the three-dimensional region in order to obtain grid density independence, as shown in table 1. This is an example of a typical grid with a high density near the plate (see Figure 4). When the number of grids in all three dimensions was adjusted, the flow field, pressure coefficient, and Nusselt number predictions were then conducted.

Table 1
The impact of the number of grid cells on the data recorded

Pin fin Model	The number of grid cells
Non Perforated	125×70×24
One Perforated	145×80×28
Two Perforated	165×88×32
Three Perforated	180×95×36
Four Perforated	200×140×48

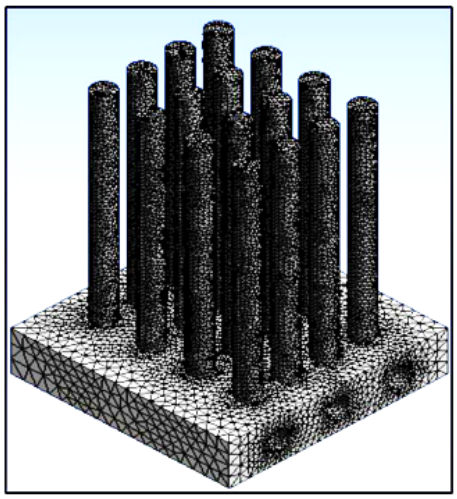

Non Perforated fin

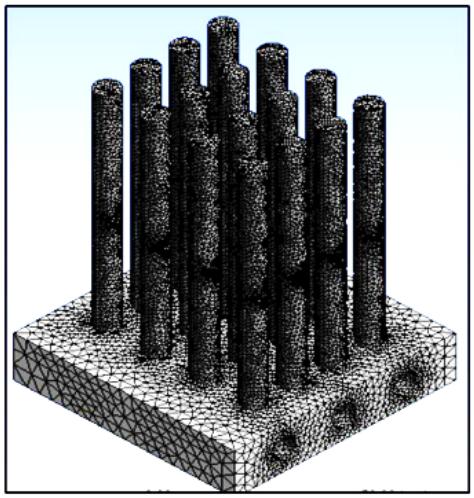

b. One Perforated fin

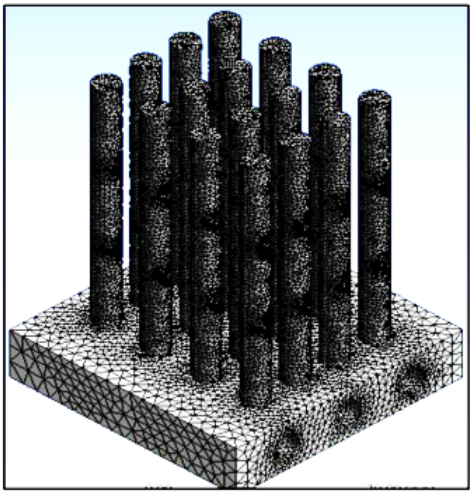

c. Two Perforated fin

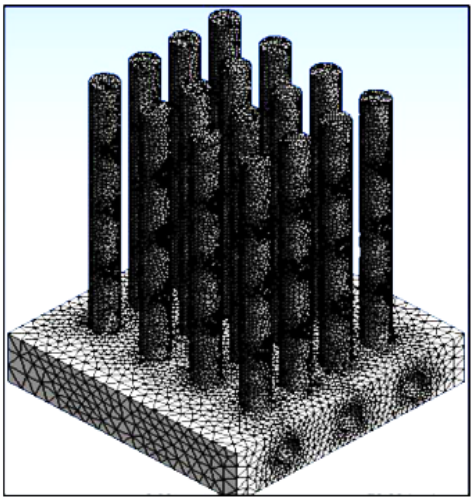

d. Three Perforated fin

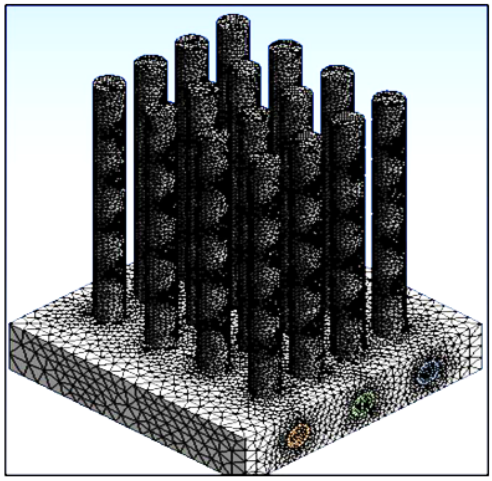

e. Four Perforated fin

Fig. 4. Computational mesh for different pin fins mesh

3.3 Boundary Conditions and Assumptions

Table 2 describes the boundary conditions and assumptions used in the CFD simulations. the pressure outlet boundary condition is set at the exit. The effects of temperature fluctuations on flow is ignored, and isothermal conditions is assumed. No slip boundary condition is applied to all tunnel walls.

Table 2
Boundary Conditions

Parameters	**Values**
Inlet air temperature (^oC)	25
Heat flux (W)	1000, 1200, 1450, 1950, 2000,2500,2700, 3200
Inlet velocity (m/s)	3
Reynolds number	14000, 26000, 41000, 52000 and 67000
Wall thickness (mm)	2
Heat generations rate	0
Convective heat transfer coefficient	From experimental result
Free stream temperature (^oC)	25
Wall motion	Stationary
Shear Boundary Conditions	No slip
Wall Roughness Constant	0.15

4. Discussion on the findings

The heat sink was numerically analyzed with solid and perforated pin fins, with varying perforation diameters. The Fluent of ANSYS 16.0 is used to select and simulate three-dimensional pin-fin array models. The temperature contours for the heat sink and fluid domain are generated and analysed. In general, it appears that the maximum temperature is reached at the heated bottom wall, which is connected to the heat sink.

Figure 5 shows the temperature distribution at constant heat power source of 600 W and constant flow rate of 3 m/s. The temperature at its base reached maximum of 69.5 ^oC and only 61 ^oC at the fin tip. The apparent temperature gradient is used for visual assistance. As can be seen in Figure 6, for the case of one perforation fin, the lowest temperature was measured at the top (52 ^oC), and the highest was recorded at the base of the fin (58 ^oC). Figure 7 depicts the temperature distribution for two perforated fins. The temperature was 48°C at the bottom and 44°C at the top, which is lower than the one perforation fin. This indicates the need of more perforation for the two perforated fins. In Figure 8, the simulation shows that the temperature distribution is different from the prior scenario, where the maximum temperature measured was 48 ^oC at the base and 39 ^oC at the top. Triple perforation is obviously superior to bilateral perforation. Figure 9 shows the temperature distribution with four perforations. The maximum temperature recorded at its base was 46°C and the maximum temperature recorded at its top was 38°C, demonstrating that the substantial temperature disparity improves heat conduction by perforation. The four-hole model also weighs 0.06 kg less than the three-hole type.

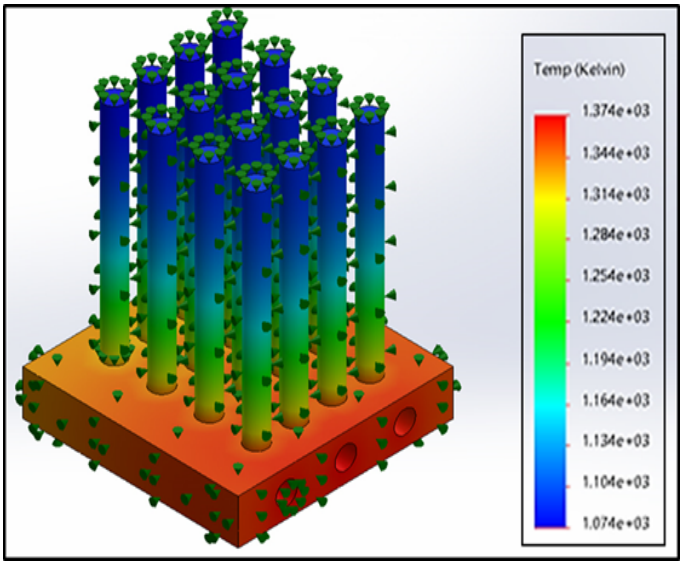

Fig. 5. Contour of temperatures for solid pin fins

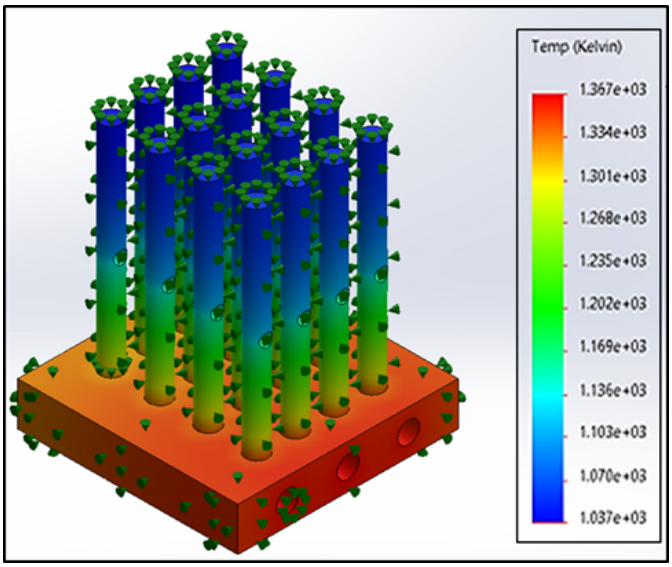

Fig. 6. Contour of temperatures for one perforated pin fin

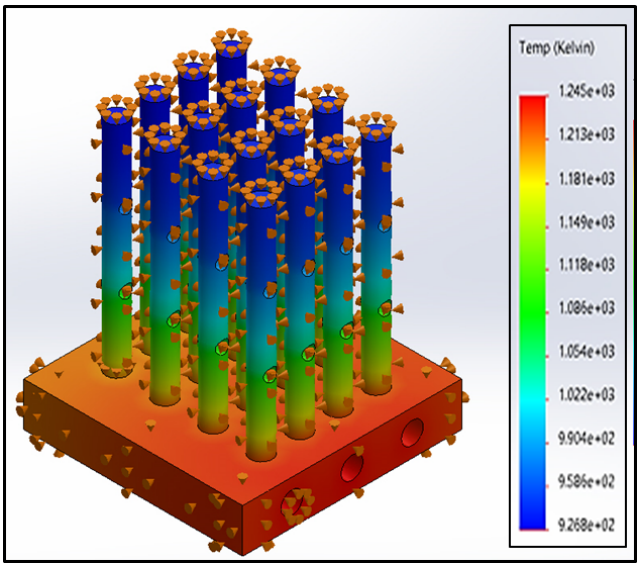

Fig. 7. Contour of temperatures for two perforations pin fin

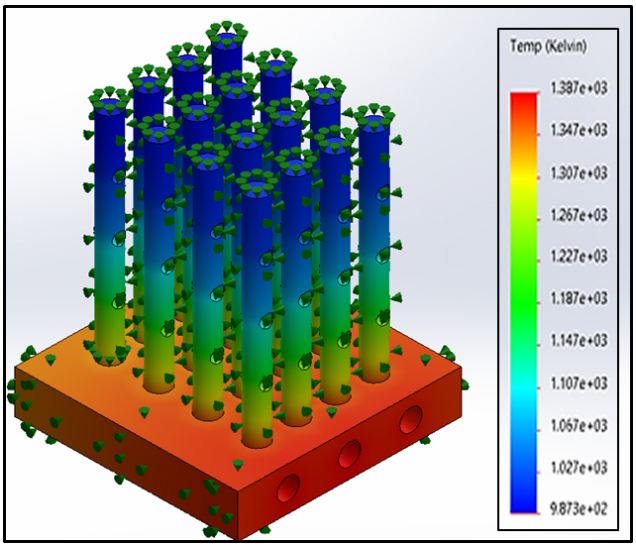

Fig. 8. Contour of temperatures for three perforations pin fin

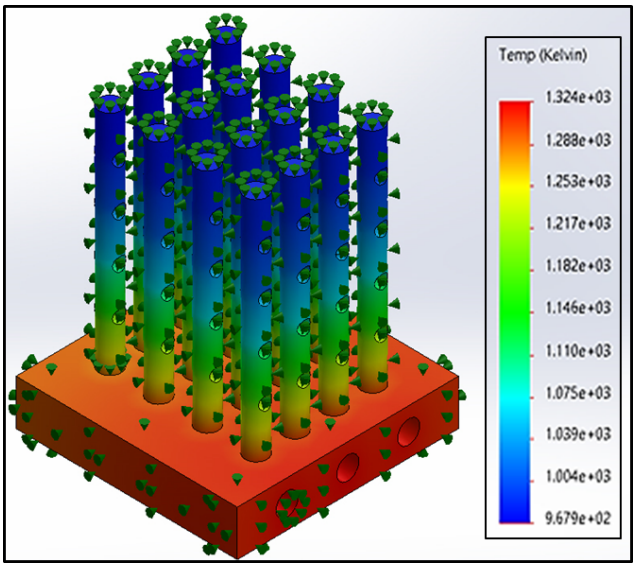

Fig. 9. Contour of temperatures for four perforations pin fin

Figure 10 shows the effect of perforation on pressure drop. Increasing the vortex currents around the fins causes the device to fail as a result of a decrease in pressure. From this graph, it can be seen that the pressure drop decreases with the number of perforations, showing that the "pumping power" drops when a solid pin fin is used and the smallest pressure drop when four perforations are used. Figure 11 shows how perforation affects the heat transfer coefficient (h). The heat transfer coefficient of a perforated fin increases in comparison to a solid fin. Solid fins have *h* value of 61.7 W/m^{2}K, whereas four-perforations have the maximum h value of 91.3 W/m^{2}K. There is a lot more heat that can pass through perforations, which makes it easier for heat to be dissipated and ensures that the device can work properly. The heat transfer performance is also affected by perforations, as shown in Figure 12. The best performance was achieved with four holes, and the worst was achieved with a solid pin fin. This indicates that the performance is inversely proportional to pressure drop (ΔP) and inversely proportional to the number of holes perforated (Nu).

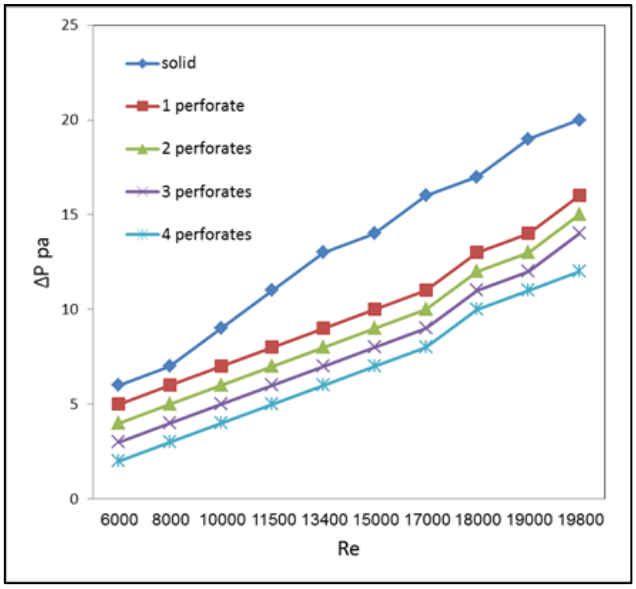

Fig. 10. The relevance of perforation in ΔP

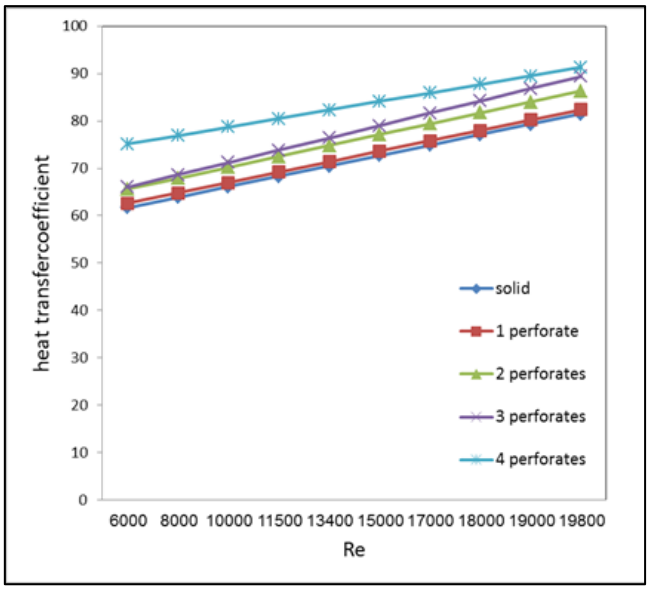

Fig. 11. The relevance of perforation in h

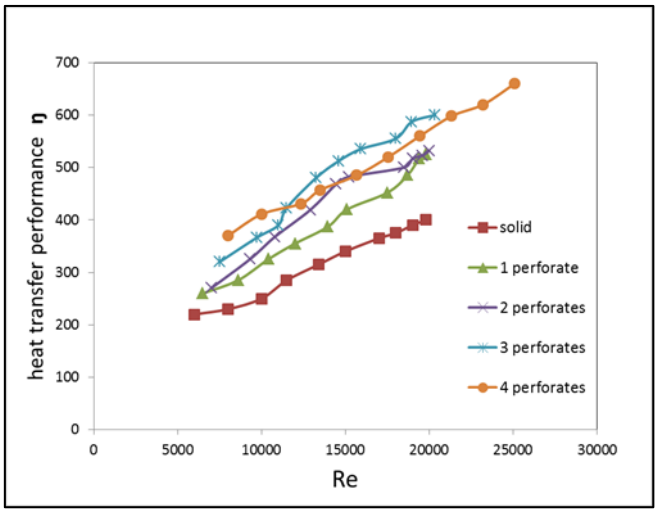

Fig. 12. The relevance of perforation in ŋ

5. Conclusion

The temperature distributions of sixteen aluminum fins were measured under a variety of forced load conditions, with perforations ranging from one to four holes upward and a fixed diameter, as well as a predetermined air supply rate of 3 m/s. The heat transfer coefficients through convection were calculated using mean temperature and empirical correlations. Following a review of the findings, a summary of the work was given below.

- Perforated pin fin heat sinks have a higher overall temperature spread than solid pin fin heat sinks.
- Perforated pin fins can provide the highest system performance if the number of perforations is optimized. Pin fins with four perforations perform best with the existing design.
- Heat sink perforation increases and reduces ΔP throughout the heat sink. Pin fin arrays with perforated holes outperform solid ones. Compared to solid pin fins, perforated pin fins use less pumping power.
- *Nu* rises in proportion to the number of perforations. Thermal dissipation is reduced when perforation is increased. Because of the holes, it caused wake reshaping and limited vertical heat transfer. Consider the number of perforations while creating an array of perforated pin fins.

References

[1] W. Al-Doori, "Enhancement of natural convection heat transfer from the rectangular fins by circular perforations," *Int. J. Automot. Mech. Eng.*, vol. 4, pp. 428–436, 2011. https://doi.org/10.15282/ijame.4.2011.5.0035

[2] T. K. Ibrahim, A. T. Al-Sammarraie, M. S. M. Al-Jethelah, W. H. Al-Doori, M. R. Salimpour, and H. Tao, "The impact of square shape perforations on the enhanced heat transfer from fins: Experimental and numerical study," *Int. J. Therm. Sci.*, vol. 149, p. 106144, 2020. https://doi.org/10.1016/j.ijthermalsci.2019.106144

[3] W. H. A. R. Al Taha, "Analysis, Performance and Optimization of Perforated and Non-Perforated Fins under Forced Convection." Sudan University of Science and Technology, 2018.

[4] W. H. A. Al Doori, "Effect of Using Various Longitudinal Fin Number In Finned Channel Heat Exchangers On Heat Flow Characteristics," *J. Adv. Res. Fluid Mech. Therm. Sci.*, vol. 53, no. 1, pp. 1–10, 2019.

[5] T. K. Ibrahim *et al.*, "Experimental and numerical investigation of heat transfer augmentation in heat sinks using perforation technique," *Appl. Therm. Eng.*, vol. 160, p. 113974, 2019. https://doi.org/10.1016/j.applthermaleng.2019.113974

[6] S. Prakash and D. Chethan, "Experimental Investigation of the Heat Transfer Rate in Perforated Fins," *Int. J. Mech. Ind. Technol.*, vol. 3, no. 2, pp. 68–72, 2016.

[7] M. Ehteshum, M. Ali, M. Q. Islam, and M. Tabassum, "Thermal and hydraulic performance analysis of rectangular fin arrays with perforation size and number," *Procedia Eng.*, vol. 105, pp. 184–191, 2015. https://doi.org/10.1016/j.proeng.2015.05.054

[8] V. S. Choure, M. R. Jagadale, and V. W. Bhatkar, "Heat Transfer Enhancement using Perforated Pin Fins," *Int. J. Technol. Res. Eng.*, vol. 3, no. 2, pp. 2347–4718, 2015.

[9] T.-M. Jeng, S.-C. Tzeng, and C.-H. Liu, "The effect of a piezoelectric fan on forced air heat transfer in a pin-fin heat sink," *Smart Sci.*, vol. 3, no. 1, pp. 1–6, 2015. https://doi.org/10.1080/23080477.2015.11665629

[10] K. H. Dhanawade, V. K. Sunnapwar, and H. S. Dhanawade, "Thermal analysis of square and circular perforated fin arrays by forced convection," *Int. J. Curr. Eng. Technol.*, vol. 2, pp. 109–114, 2014. https://doi.org/10.14741/ijcet/spl.2.2014.20

[11] W. H. Al Doori, "Numerical estimation of pressure drop and heat transfer characteristics in annular-finned channel heat exchangers with different channel configurations," *Heat Transf. Res.*, vol. 48, no. 4, pp. 1280–1291, 2019. https://doi.org/10.1002/htj.21432

[12] U. V Awasarmol and A. T. Pise, "An experimental investigation of natural convection heat transfer enhancement from perforated rectangular fins array at different inclinations," *Exp. Therm. Fluid Sci.*, vol. 68, pp. 145–154, 2015. https://doi.org/10.1016/j.expthermflusci.2015.04.008

[13] M. S. D. Bahadure and M. G. D. Gosavi, "Enhancement of natural convection heat transfer from perforated fin," *Int. J. Eng. Res.*, vol. 3, no. 9, pp. 531–535, 2014. https://doi.org/10.17950/ijer/v3s9/903

[14] H.-H. Wu, Y.-Y. Hsiao, H.-S. Huang, P.-H. Tang, and S.-L. Chen, "A practical plate-fin heat sink model," *Appl. Therm. Eng.*, vol. 31, no. 5, pp. 984–992, 2011. https://doi.org/10.1016/j.applthermaleng.2010.10.014

[15] O. N. Şara, T. Pekdemir, S. Yapici, and H. Erşahan, "Thermal performance analysis for solid and perforated blocks attached on a flat surface in duct flow," *Energy Convers. Manag.*, vol. 41, no. 10, pp. 1019–1028, 2000. https://doi.org/10.1016/S0196-8904(99)00163-6

[16] X. Yu, J. Feng, Q. Feng, and Q. Wang, "Development of a plate-pin fin heat sink and its performance comparisons with a plate fin heat sink," *Appl. Therm. Eng.*, vol. 25, no. 2–3, pp. 173–182, 2005. https://doi.org/10.1016/j.applthermaleng.2004.06.016

[17] W. H. Aldoori, A. H. Ahmed, and A. M. Ahmed, "Performance investigation of a solar water distiller integrated with a parabolic collector using fuzzy technique," *Heat Transf. Res.*, vol. 49, no. 1, pp. 120–134, 2020. https://doi.org/10.1002/htj.21602

[18] A. Yousfi, D. Sahel, and M. Mellal, "Effects of a pyramidal pin fins on CPU heat sink performances," *J. Adv. Res. Fluid Mech. Therm. Sci.*, vol. 63, no. 2, pp. 260–273, 2019.

[19] A. M. A. Elfaghi, A. A. Abosbaia, M. F. A. Alkbir, and A. A. B. Omran, "CFD Simulation of Forced Convection Heat Transfer Enhancement in Pipe Using Al2O3/Water Nanofluid," *J. Adv. Res. Numer. Heat Transf.*, vol. 8, no. 1, pp. 44–49, 2022.

[20] A. A. Khan, K. Zaimi, S. F. Sufahani, and M. Ferdows, "MHD Flow and Heat Transfer of Double Stratified Micropolar Fluid over a Vertical Permeable Shrinking/Stretching Sheet with Chemical Reaction and Heat Source," *J. Adv. Res. Appl. Sci. Eng. Technol.*, vol. 21, no. 1, pp. 1–14, 2020. https://doi.org/10.37934/araset.21.1.114

[21] S. V Patankar, *Numerical heat transfer and fluid flow*. CRC press, 2018. https://doi.org/10.1201/9781482234213

[22] P. A. Deshmukh and R. M. Warkhedkar, "Thermal performance of elliptical pin fin heat sink under combined natural and forced convection," *Exp. Therm. Fluid Sci.*, vol. 50, pp. 61–68, 2013. https://doi.org/10.1016/j.expthermflusci.2013.05.005

[23] Y. Peles, A. Koşar, C. Mishra, C.-J. Kuo, and B. Schneider, "Forced convective heat transfer across a pin fin micro heat sink," *Int. J. Heat Mass Transf.*, vol. 48, no. 17, pp. 3615–3627, 2005. https://doi.org/10.1016/j.ijheatmasstransfer.2005.03.017